

Phase-field modeling of faceted growth in solidification of alloys

Hui Xing(邢辉), Qi An(安琪), Xianglei Dong(董祥雷), and Yongsheng Han(韩永生)
Citation: Chin. Phys. B, 2022, 31 (**4**): 048104. DOI: 10.1088/1674-1056/ac3398
Journal homepage: http://cpb.iphy.ac.cn; http://iopscience.iop.org/cpb

What follows is a list of articles you may be interested in

Numerical study of growth competition between twin grains during directional solidification by using multi-phase field method

Chang-Sheng Zhu(朱昶胜), Ting Wang(汪婷), Li Feng(冯力), Peng Lei(雷鹏), and Fang-Lan Ma(马芳兰)
Chin. Phys. B, 2022, 31 (**2**): 028102. DOI: 10.1088/1674-1056/ac0eed

Modeling of microporosity formation and hydrogen concentration evolution during solidification of an Al-Si alloy

Qingyu Zhang(张庆宇), Dongke Sun(孙东科), Shunhu Zhang(章顺虎), Hui Wang(王辉), Mingfang Zhu(朱鸣芳)
Chin. Phys. B, 2020, 29 (**7**): 078104. DOI: 10.1088/1674-1056/ab8abb

A numerical study on pattern selection in crystal growth by using anisotropic lattice Boltzmann-phase field method

Zhaodong Zhang(张兆栋), Yuting Cao(曹宇婷), Dongke Sun(孙东科), Hui Xing(邢辉), Jincheng Wang(王锦程), Zhonghua Ni(倪中华)
Chin. Phys. B, 2020, 29 (**2**): 028103. DOI: 10.1088/1674-1056/ab6718

A lattice Boltzmann-cellular automaton study on dendrite growth with melt convection in solidification of ternary alloys

Dong-Ke Sun(孙东科), Zhen-Hua Chai(柴振华), Qian Li(李谦), Guang Lin(林光)
Chin. Phys. B, 2018, 27 (**8**): 088105. DOI: 10.1088/1674-1056/27/8/088105

Unifying the crystallization behavior of hexagonal and square crystals with the phase-field-crystal model

Tao Yang(杨 涛), Zheng Chen(陈铮), Jing Zhang(张静), Yongxin Wang(王永新), Yanli Lu(卢艳丽)
Chin. Phys. B, 2016, 25 (**3**): 038103. DOI: 10.1088/1674-1056/25/3/038103

Phase-field modeling of faceted growth in solidification of alloys

Hui Xing(邢辉)[1], Qi An(安琪)[1], Xianglei Dong(董祥雷)[2,†], and Yongsheng Han(韩永生)[3]

[1] *The Key Laboratory of Space Applied Physics and Chemistry, Northwestern Polytechnical University, Xi'an* 710029, *China*
[2] *College of Materials Science and Engineering, Zhengzhou University, Zhengzhou* 450001, *China*
[3] *The EMMS Group, State Key Laboratory of Multiphase Complex Systems, Institute of Process Engineering, Chinese Academy of Sciences, Beijing* 100190, *China*

(Received 24 August 2021; revised manuscript received 25 September 2021; accepted manuscript online 27 October 2021)

A regularization of the surface tension anisotropic function used in vapor-liquid-solid nanowire growth was introduced into the quantitative phase-field model to simulate the faceted growth in solidification of alloys. Predicted results show that the value of δ can only affect the region near the tip, and the convergence with respect to δ can be achieved with the decrease of δ near the tip. It can be found that the steady growth velocity is not a monotonic function of the cusp amplitude, and the maximum value is approximately at $\varepsilon = 0.8$ when the supersaturation is fixed. Moreover, the growth velocity is an increasing function of supersaturation with the morphological transition from facet to dendrite.

Keywords: faceted growth, dendrite, phase-field model

PACS: 81.30.Fb, 81.10.Aj **DOI:** 10.1088/1674-1056/ac3398

1. Introduction

Faceted growth of semiconductors such as Si, Ge and SiGe mixtures in undercooled or supersaturated melts has been attracted great interest in crystal growth field because their huge applications for electronics and photovoltaics industries.[1] It is well known that Jackson's factor α,[2] the product of the crystallographic factor and the ratio of latent heat to the rare gas constant, approximately describes the tendency of a material to facet. This has been proved in a wide range of materials.[3] Previous experimental investigations from semiconductor to intermetallic demonstrate that the faceted crystal at equilibrium could become less faceted and a transition from facet to dendrite occurs with the undercooling or supersaturation increasing.[4–6] This results from that the faceted crystal still retains tailing rough parts which can be described by a parabolic function at equilibrium. Therefore, the key point of numerical simulation of the faceted growth and its transition to dendrite is how to construct a form of anisotropic function exhibiting perfectly flat vicinal interface with rounded cusps at equilibrium. Obviously, the general form of surface tension anisotropic function cannot be used. The form of anisotropic function for facet in the presence of cusps at faceted orientations can be written as

$$a_{\mathrm{s}}(\Theta) = 1+\varepsilon\left|\Theta-\Theta_{\mathrm{f}}\right|+\cdots, \tag{1}$$

where Θ is the angle of the normal direction to the interface with respect to a fixed crystalline axis, and Θ_{f} is the orientation of a facet. Equation (1) is indeed valid for a vicinal interface when $|\Theta-\Theta_{\mathrm{f}}| \ll 1$, and ε is the cusp amplitude. As a powerful tool for simulating growth pattern selection, the phase-field method has been quantitatively and extensively used for simulating growth pattern selection in the non-faceted dendritic growth with weak and strong anisotropy from undercooled or supersaturated melts.[7–9,11] For faceted growth, it is impossible to separately treat the rough and faceted parts in the framework of the phase-field method. Hence, many attempts have been made for constructing a continuous form of surface tension anisotropic function for faceted growth.[12–17] By modifying a simple form of anisotropic function

$$a_{\mathrm{s}}(\Theta) = 1+\varepsilon\left(|\sin\Theta|+|\cos\Theta|\right) \tag{2}$$

from broken-bond model for faceted solid–gas interface, numerical simulation of the faceted dendritic growth with cusp rounding have been successfully carried out by using phase-field method by Debierre *et al.*[12] However, the modification of the anisotropy function consists of rounding the cusp over a small range of orientations

$$a_{\mathrm{s}}(\Theta) = \begin{cases} 1+\dfrac{\varepsilon}{\sin\Theta_0}-\varepsilon\left(\cot\Theta_0-1\right)\cos\Theta_0, & \Theta \le \Theta_0, \\ 1+\varepsilon\left(\sin\Theta+\cos\Theta\right), & \Theta_0 < \Theta < \dfrac{\pi}{2}-\Theta_0, \\ 1+\dfrac{\varepsilon}{\sin\Theta_0}-\varepsilon\left(\cot\Theta_0-1\right)\cos\Theta_0, & \Theta \ge \dfrac{\pi}{2}-\Theta_0, \end{cases} \tag{3}$$

[†]Corresponding author. E-mail: dxl881112@zzu.edu.cn

© 2022 Chinese Physical Society and IOP Publishing Ltd

where Θ_0 is a small but not negligible regularization range, and hence numerical results sensitively depend on the choice of Θ_0.

By using a function $\sqrt{\delta^2+x^2}$ that converges to the absolute value $|x|$ when $\delta \to 0$, a modification for Eq. (2) has been proposed by Wang *et al.*[15] in simulating vapor-liquid-solid nanowire growth, yielding

$$a_s(\Theta) = 1+\varepsilon\left(\sqrt{\delta^2+\sin^2\Theta}+\sqrt{\delta^2+\cos^2\Theta}\right). \quad (4)$$

Obviously, Eq. (4) is similar to the form given by Eq. (2) in principle, but it is a handy form to solve numerically. There is no physical meanings of the parameter δ, which is a small but not negligible constant in numerical simulation. The addition of δ to Eq. (4) allows a continuous interface stiffness. Similar form for six-fold anisotropic function was constructed by Bollada *et al.*[16] to investigate the intermetallic solidification of Al–Si alloys and the transition from faceted to dendritic morphology. In this paper, the form of Eq. (3) is adopted for studying faceted growth in solidification of a binary alloy from supersaturated melts in a two-dimensional system.

2. Method descriptions

We consider the growth of a crystal from a supersaturated alloy melt. The quantitative phase-field model for alloys solidification is developed based on the thin-interface asymptotic analysis by Karma.[18] This model can be successfully used for simulating non-faceted dendritic growth in solidification of alloys due to the inclusion of the anti-trapping current term. The phase-field variable ϕ is -1 $(+1)$ for solid (liquid) and the narrow region where it varies from -1 to $+1$ is considered as the diffusive solid–liquid interface. For alloys solidification, the solute concentration c was converted to the solute supersaturation U, which is defined as $U = ((2kc/c_0)/[1+k-(1-k)\phi]-1)/(1-k)$, where c_0 the concentration on the liquid side of the interface and k the partition coefficient. After neglecting the solute diffusion in the solid phase, governing equations for phase-field variable ϕ and solute concentration U yield

$$\begin{aligned}&\tau_\phi(\Theta)\frac{\partial\phi}{\partial t}\\ &= \nabla\cdot\left[W^2(\Theta)\nabla\phi\right]+\sum_i^{x,y}\partial_i\left[|\nabla\phi|^2\frac{\partial W^2(\Theta)}{\partial(\partial_i\phi)}\right]\\ &\quad +\phi-\phi^3-\lambda\left(1-\phi^2\right)^2U, \quad (5)\\ &\left[\frac{1+k}{2}-\frac{(1-k)\phi}{2}\right]\frac{\partial U}{\partial t}\\ &= \nabla\cdot\left[D_l\frac{1-\phi}{2}\nabla U-\boldsymbol{J}_{AT}\right]+\frac{1}{2}\left[1+(1-k)U\right]\frac{\partial\phi}{\partial t}, \quad (6)\end{aligned}$$

where $W(\Theta) = W_0 a_s(\Theta)$ and $\tau_\phi(\Theta) = \tau_0 a_s^2(\Theta)[1+(1-k)U]$, λ is the coupling constant,

$$\boldsymbol{J}_{AT} = W_0/2\sqrt{2}\left[1+(1-k)U\right]\partial_t\phi\nabla\phi/|\nabla\phi|$$

is the well-known anti-trapping current term, matched asymptotic analysis links diffusive interface width W_0 and interface attachment time scale τ_0 with capillary length d_0 and liquid diffusion coefficient D_l by $W_0 = \lambda d_0/a_1$ and $\tau_0 = \lambda a_2 W_0^2/D_l$ for vanishing interface kinetic coefficient, where $a_1 = 0.8839$ and $a_2 = 0.6267$. In this work, the modified surface tension anisotropic function Eq. (4) for faceted growth by Wang *et al.*[15] was used here. In this study, the well-characterized Si–3.5 at.% Ge alloy in solidification[19] was selected as the calculation object, and all thermophysical parameters were assumed constants which are listed as follows: average solute concentration $c_0 = 3.5$ at.%, equilibrium liquidus slope $m_l = -1.85$ K/at%, equilibrium partition coefficient $k = 0.45$, liquid diffusion coefficient $D_l = 6200$ μm^2/s, and Gibbs–Thomson coefficient $\Gamma = 0.2324$ K·μm. The coupling constant λ is selected as $\lambda = 2$ for results that are independent of the interface thickness. In numerical simulation, governing Eqs. (5) and (6) are solved by using the explicit finite difference method on a fixed grid. No-flux boundary conditions are applied to all boundaries. The numerical domain is set as 800×800. As shown in Fig. 1, the initial solid seed is introduced as a quarter of square or circle for the reason of symmetry to investigate the effect shape of initial seed of growth pattern selection.

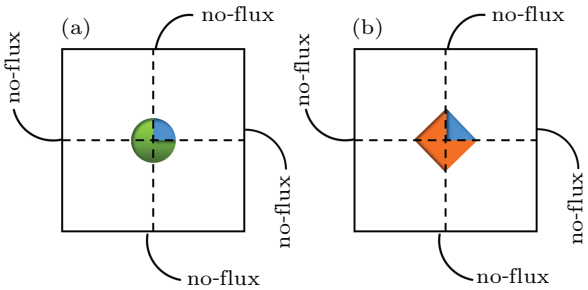


Fig. 1. Schematic of boundary conditions and initial solid seeds: (a) circl and (b) square.

3. Results and discussion

The value of δ is firstly chosen from 0.1 to 0.005 in two cases of supersaturation for a proper value of δ in numerical simulation. Solutions of Eq. (3) for δ varying from 0.1 to 0.005 are shown in Fig. 2(a). The solution of Eq. (2) has a sharp cusp at $\Theta = 0$ while solutions of Eq. (3) with finite values of δ are smooth at a small range near $\Theta = 0$. It can be seen that the profiles from Eq. (3) become convergent with the decrease in δ, which indicates that the effect of δ is only remarkably in the region near $\Theta = 0$ similar to the solution of Eq. (2) but Eq. (3) is a continuous function. In order to demonstrate the effect of δ on the crystal growth, we carried out two-dimensional phase-field simulations for various δ in two cases of supersaturation $U_0 = 0.20$ and $U_0 = 0.50$, which corresponds to square and dendritic shapes, respectively. Shapes

with solute distributions are shown in Figs. 2(b)–2(g). Obviously, phase-field simulations with Eq. (3) exhibit perfectly flat vicinal interface with rounded cusps for lower supersaturation, as shown in Fig. 2(b). Due to the growth velocity proportional to the absolute value of the supersaturation, the diffusion length for $U_0 = 0.20$ is significantly larger than that for $U_0 = 0.50$. In order to investigate the role of δ, the solid–liquid interface contours for various δ with an enlarged drawing near the tips are plotted at the same time. For lower supersaturation, as shown Figs. 2(c) and 2(d), the interface profiles for various δ overlap except the region near the tip. Clearly, the convergence with respect to δ has been achieved with the decrease of δ near the tip. For larger supersaturation, as shown in Figs. 2(f) and 2(g), the shape becomes dendritic and the difference of the interface profile for various δ becomes pronounced. Therefore, a smaller δ should be selected for larger supersaturation. The above study proves that Eq. (3) is a simple but good regularization for Eq. (2) for the cases of solidification. In the following numerical simulation, $\delta = 0.001$ are used everywhere.

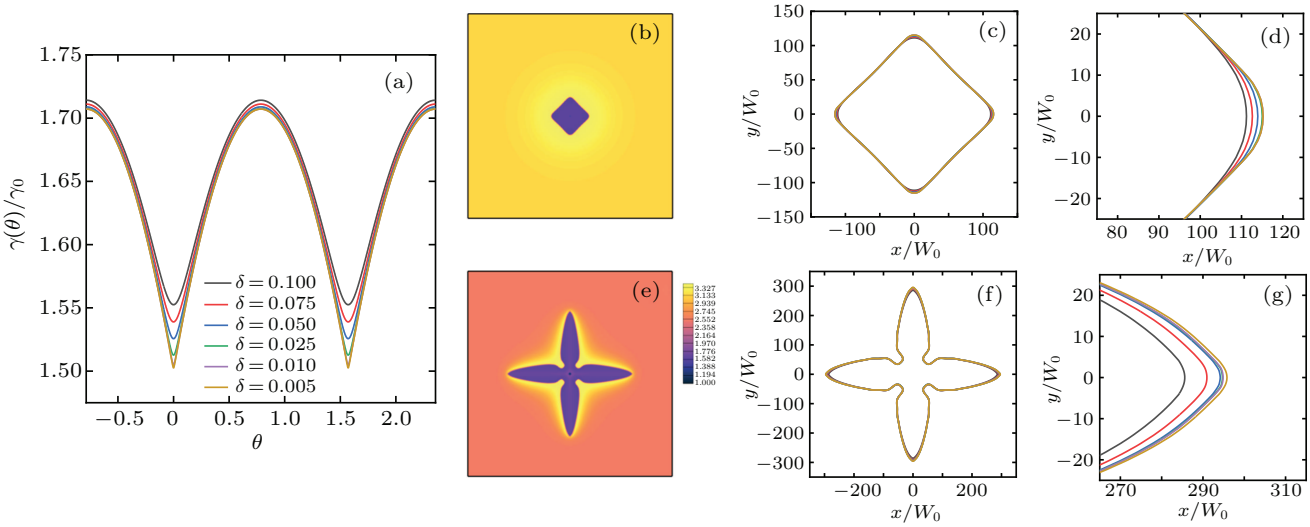


Fig. 2. (a) Solutions of the a regularization of the surface tension anisotropic function for δ varying from 0.1 to 0.005; solute distribution in square growth (b) and interface contours for various δ (c) with an enlarged drawing near the tips (d) for $U_0 = 0.20$; solute distribution in dendritic growth (e) and interface contours for various δ (f) with an enlarged drawing near the tips (g) $U_0 = 0.50$.

For faceted growth, the initial shape of the solid seed plays an important role in growth pattern selection. Two values of supersaturation $U_0 = 0.425$ and $U_0 = 0.475$ are chosen and the cusp amplitude is fixed at $\varepsilon = 0.5$, as shown in Fig. 3. It can be found that the solid–liquid interface contours from the two initial conditions overlap except the region of dendritic root for $U_0 = 0.425$. For a little higher supersaturation $U_0 = 0.475$, the square shape of the initial seed leads to a dendrite with a single tip while the circle shape results in complicated doublons shape with tip-splitting. Although the effect of initial seeds on the growth pattern selection is a numerical artifact, it is important for simulations of facet growth. This is consistent with the results from Ref. [12]. It should be noted that the doublons are symmetry-broken growth pattern with double tips that are highly dependent on the choice of the initial seed shape. The growth velocities of the leading tips with respect to the time for various initial conditions and supersaturations are presented in Fig. 3(c). Clearly, the dendrite has a higher growth velocity than doublon when the growth becomes steady. This means that the initial seed should be square to simulate faceted growth in large supersaturation or undercooling.

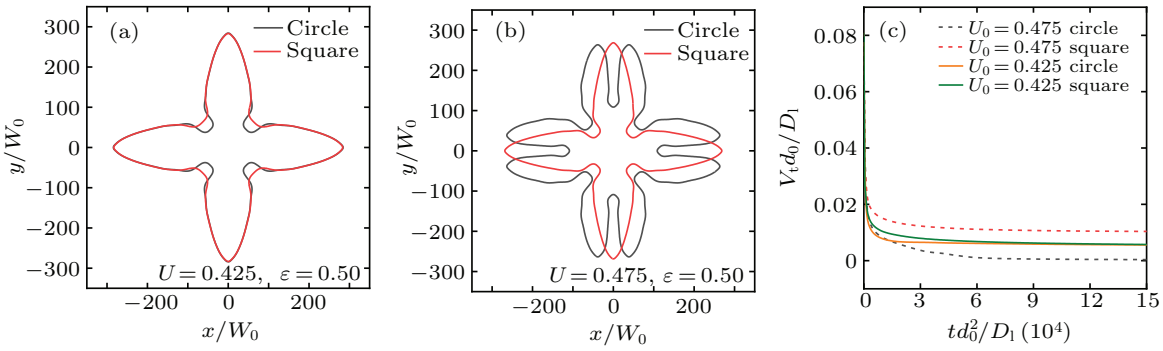


Fig. 3. Comparision of interface contours from circle and square seeds for $U_0 = 0.425$ (a) and $U_0 = 0.475$ (b); (c) temporal evolution of the leading tip velocity for various initial conditions and supersaturations.

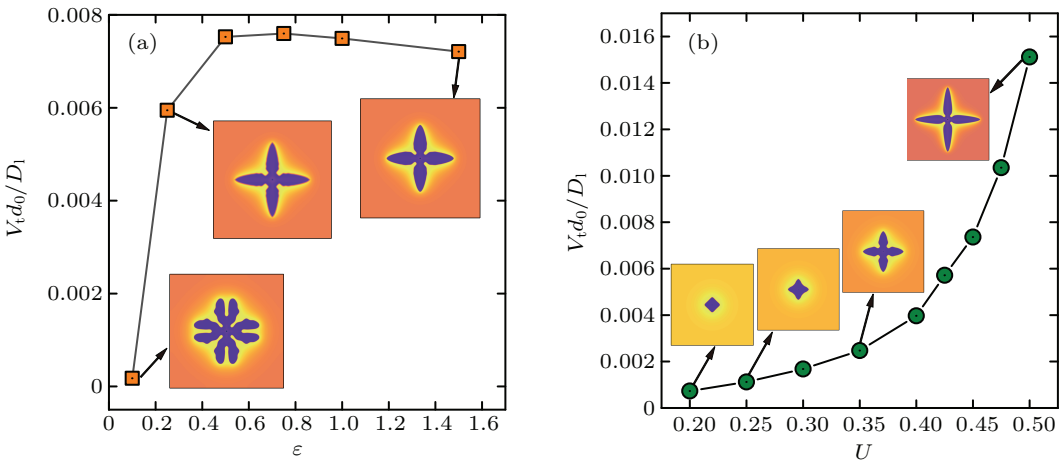


Fig. 4. (a) Steady growth velocity versus the cusp amplitude ε with typical growth patterns; (b) steady growth velocity versus supersaturation with typical growth patterns.

Now, let us focus on the effect of the cusp amplitude and supersaturation on the growth pattern selection and steady growth velocity in faceted solidification. Figure 4(a) shows the steady growth velocity versus the cusp amplitude ε with typical growth patterns for $U_0 = 0.50$. In this study, the initial shape of the solid seed is square. It can be seen that the steady growth velocity increases with the cusp amplitude for $\varepsilon \leq 0.8$. Meanwhile the growth pattern becomes from doublon to dendrite. Lower cusp amplitude means the unstable tip, and increase of the cusp amplitude results in the steady growth direction. When $\varepsilon > 0.8$, the steady growth velocity decreases with the increase of the cusp amplitude, which is consistent with the finding in Ref. [16]. As expected, the steady growth velocity is an increasing function of supersaturation when the cusp amplitude is fixed at $\varepsilon = 0.5$, which is shown in Fig. 4(b). Obviously, the morphological transition from cube to dendrite is continuous, which indicates that the transition can be quantitatively obtained from phase-field simulations by using the regularization of the anisotropic function Eq. (4).

4. Conclusion and perspectives

In this paper, the faceted growth has been numerically investigated by using a quantitative phase-field model with a regularization of the surface tension anisotropic function. The form of the anisotropic function has been used in predicting the vapor-liquid-solid nanowire growth. Results show that the value of δ can only affect the region near the tip, and the convergence with respect to δ can be achieved with the decrease in δ near the tip. And the difference of the interface profile for large supersaturation is more pronounced than that for lower supersaturation. Moreover, the initial shape of the solid seed also plays an important role in growth pattern selection for faceted growth, and the circle initial seed results in the doublon when the supersaturation is larger. The steady growth velocity is not a monotonic function of the cusp amplitude, which is consistent with the finding in Ref. [12]. The maximum value is approximately at $\varepsilon = 0.8$ when the supersaturation is fixed. Moreover, the growth velocity is a monotonic function of supersaturation, or at least in the range of the supersaturation. This study is the basis of numerical simulations of faceted growth in solidification of alloys, which proves that the form of Eq. (4) is a simply but good regularization for faceted growth in solidification of alloys. Moreover, it also can be used in the thin film growth and spiral growth in the processing of CVD.

Acknowledgements

Project supported by the National Key Research and Development Program of China (Grant No. 2018YFB2001800), the National Natural Science Foundation of China (Grant No. 21978298), the Natural Science Foundation of Shaanxi Province in China (Grant No. 2020JM-111), Applied Basic Research Key Project of Yunnan, China (Grant No. 202002AB080001-1), and Henan Youth Talent Promotion Project, China (Grant No. 2020HYTP019).

References

[1] Fujiwara K, Pan W, Usami N, *et al*. 2006 *Acta Mater.* **54** 3191
[2] Jackson K A 1984 *Mater. Sci. Eng.* **65** 7
[3] Fujiwara K, Maeda K, Usami N, *et al*. 2008 *Acta Mater.* **56** 2663
[4] Panofen C and Herlach D M 2007 *Mat. Sci. Eng. A* **449** 669
[5] Yang X B, Fujiwara K, Maeda K, *et al*. 2011 *Appl. Phys. Lett.* **98** 012113
[6] Battersby S E, Cochrane R F and Mullis A M 1997 *Mater. Sci. Eng. A* **226** 443
[7] Kuang W, Wang H, Li X, *et al*. 2018 *Acta Mater.* **159** 16
[8] Zhao Y, Zhang B, Hou H, *et al*. 2019 *J. Mater. Sci. Tech.* **35** 1044
[9] Echebarria B, Folch R, Karma A, *et al*. 2004 *Phys. Rev. E* **70** 061604
[10] Xing H, Dong X L, Sun D K, *et al*. 2020 *J. Mater. Sci. Tech.* **57** 28
[11] Zhang J, Wang H, Kuang W, *et al*. 2018 *Acta Mater.* **148** 86
[12] Debierre J M, Karma A, Celestini F, *et al*. 2003 *Phys. Rev. E* **68** 041604
[13] Chen P, Tsai Y and Lan C 2008 *Acta Mater.* **56** 4114
[14] Chen G, Lin H and Lan C 2016 *Acta Mater.* **115** 324
[15] Wang N, Upmanyu M and Karma A 2018 *Phys. Rev. Mater.* **2** 033402
[16] Bollada P, Jimack P and Mullis A 2018 *Compu. Mater. Sci.* **144** 76
[17] Stefan-Kharicha M, Kharicha A, Zaidat K, *et al*. 2020 *J. Crys. Growth* **541** 125667
[18] Karma A 2001 *Phys. Rev. Lett.* **87** 115701
[19] Lin H, Chen H and Lan C 2014 *J. Crys. Growth* **385** 44